Cell J
Open Access
doi: 10.22074/cellj.2026.2066514.1886
Cell Journal (Yakhteh)
https://celljournal.org
Original Article
Vol 27, 2025; 1886

Therapeutic Efficacy of Adipose-Derived Stem Cells for Bleomycin-Induced Idiopathic Pulmonary Fibrosis: A Comparative Study of Intravenous versus Intratracheal Administration

Yan-Yan Ng, M.D.[1], Chen-Yu Chiang, Ph.D.[2, 3], Yung-Lun Ni, M.D.[4], Huan-Ting Shen, Ph.D.[4], Chien-Ying Lee, Ph.D.[2, 3], Tai-Ping Lee, Ph.D.[5], Martin Sieber, Ph.D.[5], Ching-Chi Tseng, M.D.[6, 7], Chang-Yao Thomas Tsao, Ph.D.[8*], Yu-Hsiang Kuan, Ph.D.[2, 3*]

1. Department of Pediatric, Chung Kang Branch, Cheng Ching Hospital, Taichung, Taiwan
2. Department of Pharmacology, School of Medicine, Chung Shan Medical University, Taichung, Taiwan
3. Department of Pharmacy, Chung Shan Medical University Hospital, Taichung, Taiwan
4. Department of Pulmonary Medicine, Taichung Tzu Chi Hospital, Buddhist Tzu Chi Medical Foundation, Taichung, Taiwan
5. BIONET Therapeutics Corp., Taipei 11497, Taiwan
6. Department of Dermatology, The Wilshire Lab and Aesthetic Clinic, Shenzhen, China
7. Department of Dermatology, Shiso Municipal Hospital, Hyogo, Japan
8. Division of Chest, Department of Internal Medicine, Chung Shan Medical University Hospital, Taichung, Taiwan

Abstract

Objective: To compare the therapeutic effects of intravenous (IV) and intratracheal (IT) delivery of adipose-derived stem cells (ADSCs) in a mouse model of bleomycin (BLM)-induced idiopathic pulmonary fibrosis (IPF).

Materials and Methods: In this experimental study, BALB/c mice were divided into 4 groups: control, BLM only, BLM+ADSC(IV), BLM+ADSC(IT). ADSCs were administered on day 14 after BLM induction. Outcomes measured on day 42 included mortality, body weight, lung edema, collagen deposition, fibrosis scoring, cytokine levels (TGF-β, SDF-1, IL-6, IL-1β, TNF-α), hydroxyproline, and leukocyte infiltration.

Results: ADSC(IT) reduced mortality more effectively than ADSC(IV). Both IV and IT mitigated weight loss and lung edema with no significant difference. Both routes significantly decreased collagen synthesis, collagen fiber accumulation, Ashcroft scores, and hydroxyproline levels. Both routes lowered TGF-β, α-SMA, TNF-α, IL-6, IL-1β, and SDF-1 levels, and reduced leukocyte infiltration and alveolar barrier dysfunction, with no significant difference between routes.

Conclusion: This design enables discrimination between route-dependent and route-independent therapeutic effects of ADSCs, thereby providing new insight into the optimization of stem cell delivery strategies for pulmonary fibrosis. Importantly, whether the choice of delivery route differentially affects survival and inflammatory resolution, independent of antifibrotic efficacy, remains insufficiently addressed in current preclinical studies.

Keywords: Collagen Remodeling, Idiopathic Pulmonary Fibrosis, Mesenchymal Stem Cells

Citation: Ng YY, Chiang CY, Ni YL, Shen HT, Lee CY, Lee TP, Sieber M, Tseng CC, Tsao TC, Kuan YH. Therapeutic efficacy of adipose-derived stem cells for bleo-mycin-induced idiopathic pulmonary fibrosis: a comparative study of intravenous versus intratracheal administration. Cell J. 2025; 27: 1886. doi: 10.22074/cellj.2026.2066514.1886
This open-access article has been published under the terms of the Creative Commons Attribution Non-Commercial 3.0 (CC BY-NC 3.0).

Introduction

Idiopathic pulmonary fibrosis (IPF) is a severe and progressive lung disease associated with high morbidity and mortality in numerous countries (1, 2). The pathogenesis of IPF is multifaceted and has yet to be elucidated (1-3). IPF is characterised by chronic inflammation, oxidative stress, and aberrant wound healing that ultimately result in irreversible lung damage (1, 3). This disease generally involves excessive accumulation of extracellular matrix components, predominantly collagen, and increased interstitial fibrosis, which lead to lung function decline (3, 4). These pathological features are caused by scarring of

Royan Institute
Cell Journal (Yakhteh)

Received: 21/July/2025, Revised: 12/February/2026, Accepted: 23/February/2026
*Corresponding Addresses: Division of Chest, Department of Internal Medicine, Chung Shan Medical University Hospital, Taichung, Taiwan
Department of Pharmacology, School of Medicine, Chung Shan Medical University, Taichung, Taiwan
Emails: tcyt@csmu.edu.tw, kuanyh@csmu.edu.tw

lung tissue and restructuring of the interstitium, distal airway, and alveolar spaces (3, 4). IPF can be initiated by exposure to various toxins, by radiation exposure through inhalation of various compounds, or by infection (3, 4). Treatment strategies that are effective against IPF have only recently become available (1, 4).

Bleomycin (BLM) is often used to induce IPF in animals in research regarding the disease (5). Intratracheal (IT) administration of BLM leads to increased production of proinflammatory cytokines and chemokines, namely interleukin-1β (IL-1β), IL-6, tumor necrosis factor-alpha (TNF-α), transforming growth factor-beta (TGF-β), and stromal cell-derived factor 1 (SDF-1), by pulmonary tissue, which disrupts the integrity of the pulmonary endothelial barrier (6, 7). Subsequently, pulmonary immune responses are mediated. That is, various leukocytes are recruited, including innate and adaptive white blood cells (8, 9).

In recent decades, remarkable progress has been made in regenerative medicine, particularly in stem cell-based therapy (10). This innovative treatment approach involves leveraging the regenerative properties of stem cells to promote tissue regeneration and cellular replacement (10). In stem cell-based therapy, various types of viable human stem cells are used to treat diseases. Mesenchymal stem cells derived from different tissue sources, including bone marrow and umbilical cord, have demonstrated immunomodulatory and antifibrotic potential in experimental lung injury models. Among these sources, adipose-derived stem cells (ADSCs) offer practical advantages for translational application, such as higher cell yield, less invasive harvesting procedures, and preserved paracrine activity, which support their selection in the present study. ADSCs are among these cells and have emerged as a valuable component of such therapy. ADSCs originate from the stromal vascular fraction of adipose tissue, and they are primarily sourced from perivascular adipose tissue, including that of subcutaneous fat deposits (11). IT administration of ADSCs was reported to enhance recovery from IPF in Sprague-Dawley rats with pulmonary fibrosis induced using BLM (11). The transplantation of ADSCs into the airways was determined to considerably decrease the rate of fibrosis by altering the levels of Hsp27, Vegfa, Nf-kβ, Il-6, Col4, and Tgf-β1. Such transplantation is effective in both the early and established stages of the disease (12). Moreover, introducing ADSCs into the lungs through intravenous (IV) administration in the early stage of this disease can mediate the repair of lung injuries and can reduce lung fibrosis (13). This approach may be effective for treating lung diseases in their initial stages, as indicated by studies on IPF caused by BLM (13). In consideration of the aforementioned findings, the present study conducted a comparative analysis of IV and IT administration of ADSCs in mice with BLM-induced IPF in the established stage. Unlike previous studies that evaluated a single delivery route or different experimental time windows, this study directly compares IV and IT administration under identical experimental conditions, including the same disease stage, cell source, dosage, and outcome measures.

Materials and Methods

Isolation and culture of human adipose-derived stem cells

Human ADSCs were obtained from BIONET (Taipei City, Taiwan). These ADSCs were cultured in the BIONET Laboratory under Good Manufacturing Practice conditions, as described in a previous study (14).

Animals

Male BALB/c mice aged 7 to 8 weeks that were obtained from BioLASCO Taiwan (Taipei City, Taiwan) were bred in a pathogen-free facility at the Animal Science Center of Chung Shan Medical University (Taichung, Taiwan). The mice were housed in cages at an ambient temperature of 23°C to 25°C and with humidity maintained at 30-70%. They were provided with a standard laboratory diet and had unrestricted access to water.

Institutional review board statement

The study was conducted according to the guidelines of the Declaration of the International Animal Care and Use Committee (IACUC). It was approved by the Institutional Animal Ethics Committee of Chung Shan Medical University (Approval No. 2429).

Animal experiment design

This study assessed the potential of ADSCs for treating BLM-induced pulmonary fibrosis in a rodent model. The experiment involved 4 groups. Each group received different treatments that were used to evaluate the effectiveness of ADSCs administered through different routes. The 80 mice that were used in this study were randomly divided into the following 4 groups, with 20 mice in each group: control group: these mice received IT-administered saline on days 0 and 14; BLM group: these mice received IT-administered BLM at 5 mg/kg on day 0; ADSC(IT) group: these mice received IT-administered BLM on day 0, with this followed by IT administration of 1×10^6 ADSCs on day 14; and ADSC(IV) group: these mice received IT-administered BLM on day 0, with this followed by IV administration of 1×10^6 ADSCs on day 14. All mice were euthanised on day 42, and their lung tissues and bronchoalveolar lavage fluid (BALF) were collected for histological, biochemical, and molecular analyses for assessing fibrosis, proinflammatory responses, and immunocyte infiltration. Due to mortality during the experimental period, the number of animals available for endpoint analyses varied among groups; therefore, equal numbers of surviving animals (n=6 per group) were randomly selected for biochemical and histological assays. No additional immunosuppressive agents were administered, as ADSCs are known to possess low immunogenicity and exert therapeutic effects primarily through paracrine immunomodulation (25).

Mortality, body weight, lung oedema, and pulmonary index analysis of mice

After inducing pulmonary fibrosis by using BLM, we monitored the mortality of the animals for 42 days. We confirmed that the animals had died by assessing their heartbeats, respiration, eye reflexes, and body movement. We weighed all animals in all groups before and after inducing pulmonary fibrosis. We also determined the wet weight of the lung tissues after excision and measured the dry weight of the tissues after placing the wet lung tissues in an oven set to 80°C for 48 hours. Lung oedema was assessed using the wet/dry weight ratio, which was calculated by dividing the dry weight by the wet weight. Additionally, we calculated the pulmonary index by dividing the body weight by the wet lung weight (15, 16).

Bronchoalveolar lavage fluid collection and cell counting

Following 42-day treatment with BLM, the mice were anesthetised. Subsequently, the bronchoalveolar lavage (BAL) procedure was performed; the mice were administered 3 sequential lavages of 1 mL of ice-cold sterile saline through a tracheal cannula. The supernatants obtained after centrifugation were used for quantification of the levels of proinflammatory cytokines and the mediators of lung fibrosis. The cellular fraction was resuspended, and cell counting was conducted through haemocytometry. Furthermore, cell subsets were identified using flow cytometry. Specifically, neutrophil subsets were characterised on the basis of the expression of CD45 and Ly6G. Moreover, lymphocyte subsets were identified on the basis of the expression of CD45 and CD3, and phagocyte subsets (neutrophils, monocytes, and macrophages) were identified on the basis of the expression of CD45 and CD11b (17, 18).

Histopathological analysis

After BLM treatment, on day 42, the lungs of each mouse were isolated and fixed in 10% neutral buffered formalin. Subsequently, the lungs were embedded in paraffin, sectioned, and stained with either haematoxylin and eosin (H&E) or Masson's trichrome stain. The lung sections were evaluated for fibrotic changes by using a microscope. Fibrotic changes in 10 fields of each slide were assessed, and these changes were assigned a score ranging from 0 to 8 based on the Ashcroft scoring system, where 0 indicates normality and 8 indicates severe fibrosis. The fibrotic areas in each field were analysed, and the total field area was computed and is expressed as a fraction of 100%.

Immunohistochemical analysis

In preparation for immunohistochemical staining, the lung tissue sections underwent dewaxing and dehydration (18, 19). Antigen retrieval was performed by using antigen retrieval buffer to expose antigens. Hydrogen peroxide was applied to block endogenous peroxidase activity, and the slides were incubated with antibodies for TNFα and α-SMA, a smooth muscle-specific marker. Subsequently, the slides were incubated with a horseradish peroxidase-labelled donkey anti-rabbit or anti-mouse secondary antibody at room temperature. Finally, the slides were visualised using 3,3'-Diaminobenzidine reagents and viewed under the Lionheart-FX automated microscopy (Agilent Technologies, Santa Clara, CA, USA).

Enzyme-linked immunosorbent assay

The levels of hydroxyproline, stromal-derived growth factor-1 (SDF-1), and TGF-β in the lung tissues were assessed through enzyme-linked immunosorbent assay (ELISA). The frozen lung tissues were homogenised, and the resulting lysates were centrifuged at 5000 ×g for 10 minutes at 4°C. The levels of hydroxyproline, SDF-1, and TGF-β in the supernatants were quantified using ELISA kits. Additionally, the levels of TNF-α, IL-1β, and IL-6 levels in BALF were determined using ELISA kits (16, 17). All ELISA procedures were performed following the manufacturer's instructions.

Statistical analysis

The data values were reported as the mean ± standard deviation (SD). Statistical significance between groups was assessed using a one-way analysis of variance (ANOVA), and pairwise comparisons between multiple groups were conducted using Fisher's least significant difference (LSD) test. Statistical significance was defined as $P<0.05$; however, when P values were extremely small, results were reported as $P\leq0.001$. Mortality rates were analyzed using the Kaplan-Meier method, and survival curves were compared using the log-rank test while pairwise comparisons were conducted. Data were allocated into four groups, including control, Bleomycin, ADSC (IV)+Bleomycin, and ADSC(IT)+Bleomycin. Exact P values for log-rank comparisons are reported in Figure 1.

Results

Effects of ADSCs on mortality and body weight in mice with BLM-induced pulmonary fibrosis

To elucidate the protective effects of ADSCs administered through IV or IT routes on mortality, this study administered ADSC treatment to mice with BLM-induced pulmonary fibrosis through either IV or IT routes on day 14 post-BLM exposure. The mortality rates were assessed on a daily basis for 42 days. Kaplan-Meier survival analysis and then compared using the log-rank test revealed a marked survival deficit following BLM challenge (Fig.1A). Relative to Control, the BLM group showed an early and sustained separation of the survival curve, consistent with increased mortality over the observation period (P=0.006). ADSC(IT) (P=0.014) and ADSC(IV) (P=0.014) regimens shifted the Kaplan-Meier curves upward compared with BLM alone, indicating improved survival. Notably, the IT-treated cohort exhibited a more favorable survival trajectory than the IV-treated cohort, supporting an apparent advantage of IT delivery for improving survival in this model. The results indicated that

the administration of ADSCs mitigated the loss of body weight caused by BLM treatment. Notably, the reduction in body weight loss following IV administration of ADSCs was comparable to that observed following IT administration (Fig.1B).

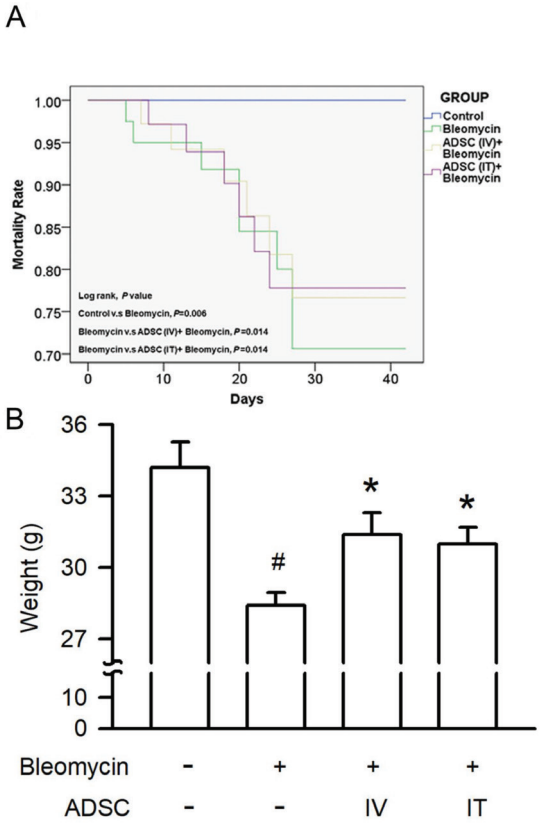


Fig.1: Effects of ADSC on mortality and body weight in BLM-induced pulmonary fibrosis. **A.** Kaplan-Meier curves were generated for control, BLM, ADSC(IV)+BLM, and ADSC(IT)+BLM groups (42 days per group). Group differences were assessed using the log-rank test, with pairwise comparisons performed under a stratified framework based on the stratification variable. Exact log-rank P values are shown. **B.** The plot illustrated the body weights. Data are presented as mean ± SD (n=6 per group). Statistical significance was assessed using one-way ANOVA followed by Fisher's LSD test. The symbol # denoted a significant difference between the indicated group and the control group, while * indicated a significant difference between the indicated group and the BLM group, with P<0.05. ADSC; Adipose-derived stem cells, IV; Intravenous, IT; Intratracheal, and BLM; Bleomycin.

Effects of ADSCs on lung oedema and collagen synthesis in mice with BLM-induced pulmonary fibrosis

The lung index and wet/dry weight ratio are indicators of lung oedema. As presented in Figure 2, lung oedema in the BLM group was significantly increased relative to that in the control group (P≤0.001). Furthermore, lung oedema in the ADSC(IV) and ADSC(IT) groups was significantly decreased relative to that in the BLM group (P≤0.001). However, no significant difference was noted between the ADSC(IV) and ADSC(IT) groups. In addition, collagen synthesis in the BLM group was significantly increased relative to that in the control group (P≤0.001), and collagen synthesis in the ADSC(IV) and ADSC(IT) groups was significantly decreased relative to that in the BLM group (P≤0.001). However, no significant difference was observed between the ADSC(IV) and ADSC(IT) groups.

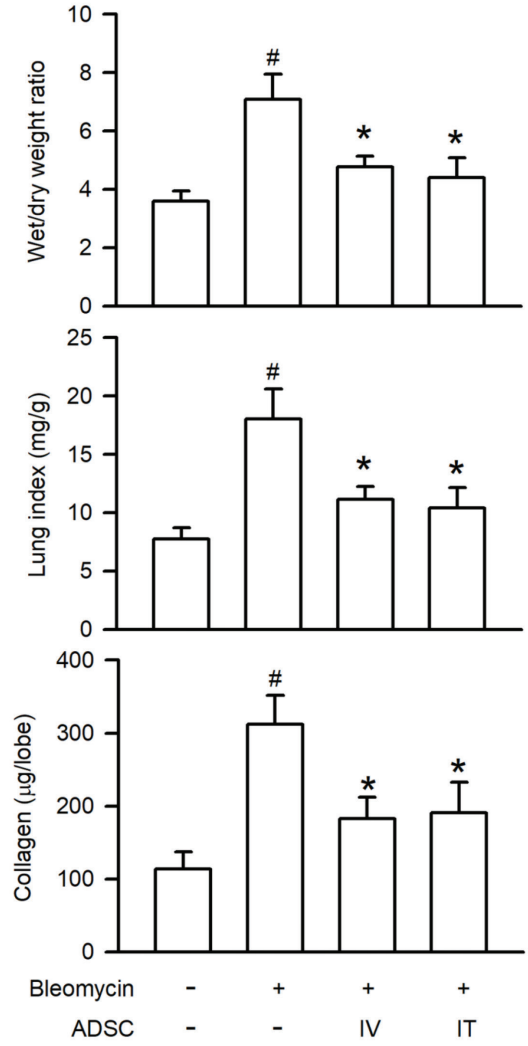


Fig.2: Effects of ADSC on lung edema and collagen synthesis in bleomycin-induced pulmonary fibrosis. The parameters illustrated were lung index, wet/dry weight ratio, and collagen synthesis. Data are presented as mean ± SD (n=6 per group). Statistical significance was assessed using one-way ANOVA followed by Fisher's LSD test. The symbol # denoted a significant difference between the indicated group and the control group, while * indicated a significant difference between the indicated group and the BLM group, with P≤0.001. ADSC; Adipose-derived stem cells, IV; Intravenous, IT; Intratracheal, and BLM; Bleomycin.

Effects of ADSCs on histopathological changes and fibrotic lesions in lungs of mice with BLM-induced pulmonary fibrosis

Figure 3 presents the histopathological morphology of lung tissues with H&E and Masson's trichrome staining in mice with BLM-induced pulmonary fibrosis. H&E staining revealed that the control group had healthy pulmonary architecture, preserved alveolar walls, and clear lumens without leukocyte infiltration. BLM-induced pulmonary fibrosis caused lung tissue degradation, which was characterised by disrupted alveolar walls, leukocyte infiltration, and localised haemorrhage. The ADSC(IV) and ADSC(IT) groups exhibited significantly improved histopathological morphologies, as indicated by H&E staining and Ashcroft scores (P≤0.001). No significant difference

was observed between the ADSC(IV) and ADSC(IT) groups. Masson's staining indicated that the control group exhibited evenly distributed colours without noticeable fibrotic lesions. By contrast, the BLM-treated group exhibited severe fibrotic lesions with the substantial accumulation of collagen fibres; the accumulation was notable in the interstitial areas surrounding the bronchial and vascular branches of the lung. The ADSC(IV) and ADSC(IT) groups exhibited a significant reduction in collagen fibre proliferation and accumulation, as indicated by Masson's staining and fibrotic area analysis (P≤0.001). Additionally, no discernable difference was noted in the effects of ADSCs on the histopathological changes that occurred between the ADSC(IV) and ADSC(IT) groups.

Effects of ADSCs on TGF-β, a-SMA, and hydroxyproline levels in lungs of mice with BLM-induced pulmonary fibrosis

TGF-β is a key driver of pulmonary fibrotic processes. Therefore, this study examined the effect of BLM treatment on TGF-β levels. Immunohistochemistry and ELISA revealed that BLM led to marked increases in TGF-β levels relative to those in the control group (P≤0.001). In addition, the ADSC(IV) and ADSC(IT) groups exhibited significantly decreased levels of TGF-β relative to the BLM group (P≤0.001, Fig.4A). Elevated α-SMA levels are indicative of fibroblast activation, which leads to fibrosis (20). In addition, this study investigated the effect of BLM on α-SMA levels. Immunohistochemistry revealed that BLM led to marked increases in α-SMA levels relative to those the control group (P≤0.001, Fig.4B). Furthermore, the ADSC(IV) and ADSC(IT) groups exhibited significantly decreased α-SMA levels relative to those in the BLM group (P≤0.001). Hydroxyproline is commonly used as a biochemical marker to quantify the collagen content in fibrotic tissue (21). Therefore, this study evaluated the effect of BLM treatment on hydroxyproline levels. ELISA revealed that BLM led to marked increases in hydroxyproline levels relative to those in the control group. In addition, the ADSC(IV) and ADSC(IT) groups exhibited significantly decreased hydroxyproline levels relative to those in the BLM group (P≤0.001, Fig.4C). However, no significant differences were observed in the effects of ADSCs on TGF-β, α-SMA, and hydroxyproline levels between the ADSC(IV) and ADSC(IT) groups.

Effects of ADSCs on TNF-a, SDF-1, IL-6, and IL-1β levels in mice with BLM-induced pulmonary fibrosis

To explore the effects of ADSCs on cytokine levels in mice with BLM-induced pulmonary fibrosis, this study analysed the presence of inflammatory cytokines, including TNF-β, SDF-1, IL-6, and IL-1 β, in BALF through ELISA. The results revealed that BLM treatment led to marked increases in the levels of inflammatory cytokines relative to those in the control group (P≤0.001). Furthermore, the ADSC(IV) and ADSC(IT) groups exhibited significantly decreased levels of cytokines relative to those in the BLM group (P≤0.001, Fig.5). However, no significant differences were observed in the effects of ADSCs on the cytokine levels between the ADSC(IV) and ADSC(IT) groups.

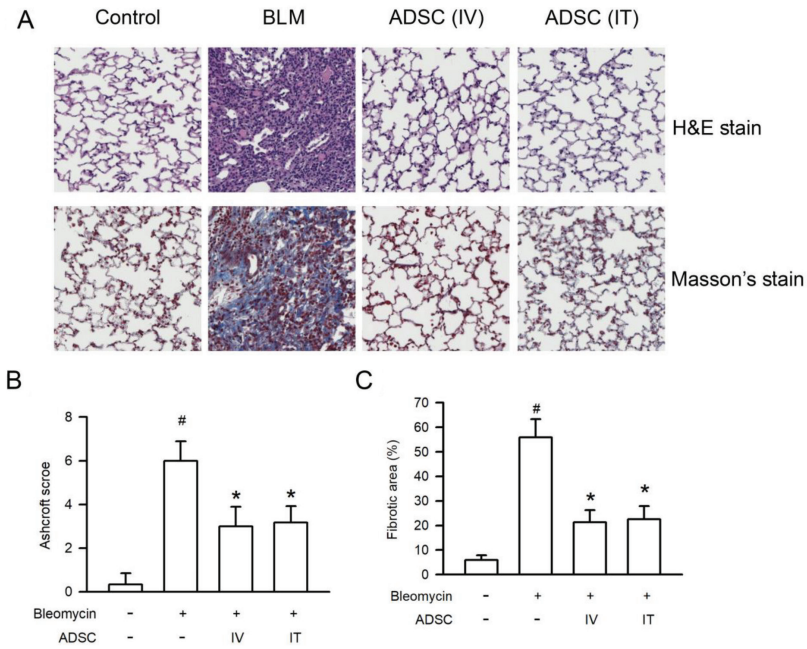


Fig.3: Effects of ADSC on the histopathological exchange and fibrotic lesion of lungs in bleomycin-induced pulmonary fibrosis. **A.** The plot illustrated the histopathological morphology of lung tissues with H&E and Masson's trichrome staining assay. The parameters illustrated were **B.** Ashcroft score and **C.** Fibrotic areas. Data are presented as mean ± SD (n=6 per group). Statistical significance was assessed using one-way ANOVA followed by Fisher's LSD test. The symbol # denoted a significant difference between the indicated group and the control group, while * indicated a significant difference between the indicated group and the bleomycin group, with P≤0.001. ADSC; Adipose-derived stem cells, H&E; Haematoxylin and eosin, IV; Intravenous, and IT; Intratracheal.

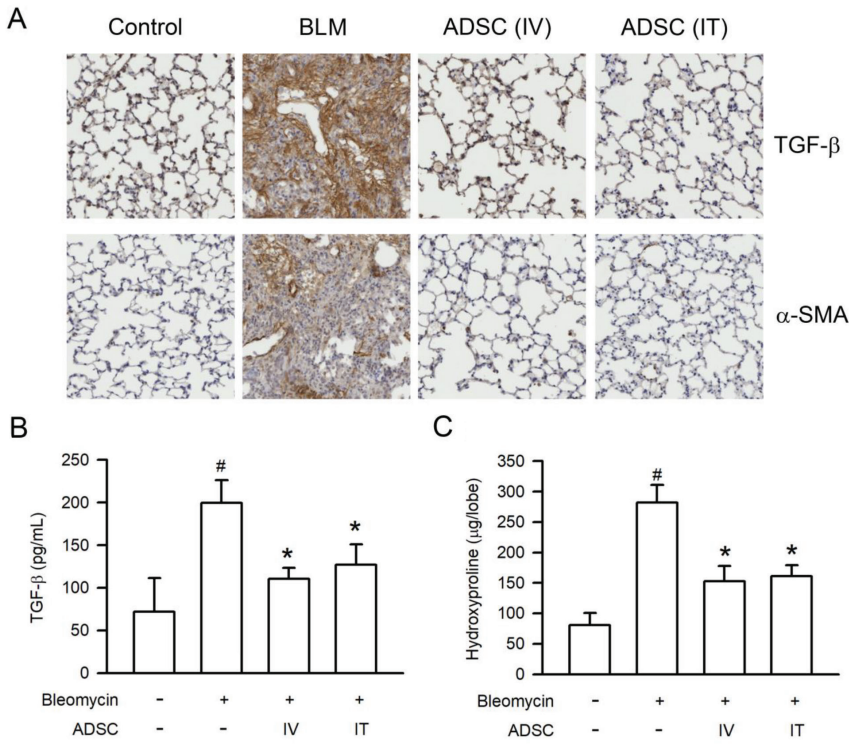


Fig.4: Effects of ADSC on the expression of TGF-β, α-SMA, and hydroxyproline of lungs in bleomycin-induced pulmonary fibrosis. **A.** The plot illustrated the histopathological morphology of lung tissues using an immunohistochemistry staining assay. The parameters illustrated were **B.** TGF-β and **C.** Hydroxyproline levels. Data are presented as mean ± SD (n=6 per group). Statistical significance was assessed using one-way ANOVA followed by Fisher's LSD test. The symbol # denoted a significant difference between the indicated group and the control group, while * indicated a significant difference between the indicated group and the bleomycin group, with P≤0.001. ADSC; Adipose-derived stem cells, IV; Intravenous, IT; Intratracheal, TGF-β; Transforming growth factor-beta, α-SMA; Stromal cell-derived factor 1, and BLM; Bleomycin.

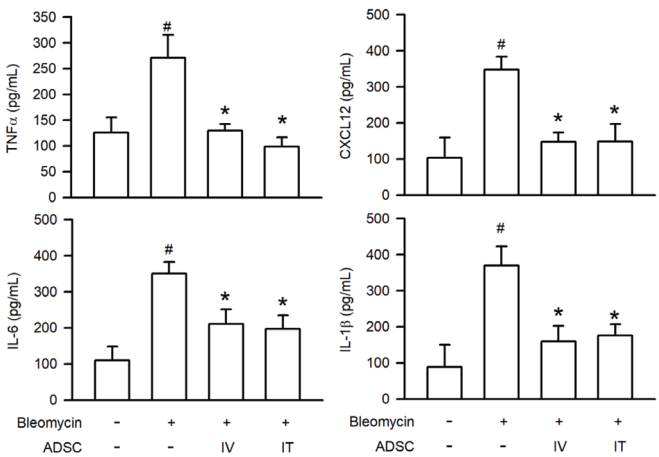


Fig.5: Effects of ADSC on the secretion of TNF-β, SDF-1, IL-6, and IL-1β in bleomycin-induced pulmonary fibrosis. The parameters illustrated were TNF-β, SDF-1, IL-6, and IL-1β. Data are presented as mean ± SD (n=6 per group). Statistical significance was assessed using one-way ANOVA followed by Fisher's LSD test. The symbol # denoted a significant difference between the indicated group and the control group, while * indicated a significant difference between the indicated group and the bleomycin group, with P≤0.001. ADSC; Adipose-derived stem cells, IV; Intravenous, IT; Intratracheal, TNF-β; Tumor necrosis factor-alpha, SDF-1; Stromal cell-derived factor 1, and IL; Interleukin.

Effects of ADSCs on alveolar barrier dysfunction and leukocyte infiltration in mice with BLM-induced pulmonary fibrosis

Leukocyte infiltration has been indicated to occur during the onset and progression of pulmonary fibrosis due to disruptions in the alveolar barrier (22). Therefore, the present study investigated the effect of BLM on alveolar barrier dysfunction. The Bradford protein assay revealed that BLM treatment led to marked increases in protein concentrations in BALF relative to those in the control group (P≤0.001). Furthermore, the ADSC(IV) and ADSC(IT) groups exhibited significantly decreased protein concentrations in BALF relative to those in the BLM group (P<0.05, Fig.6). This study further investigated the effect of BLM on leukocyte infiltration. Flow cytometry revealed that BLM treatment led to marked increases in the infiltration of leukocytes, including neutrophils and lymphocytes, relative to that in the control group (P≤0.001). In addition, the ADSC(IV) and ADSC(IT) groups exhibited significantly decreased leukocyte infiltration relative to that in the BLM group (P≤0.001, Fig.6). However, no significant differences were identified in the effects of ADSCs on alveolar barrier dysfunction and leukocyte infiltration between the ADSC(IV) and ADSC(IT) groups.

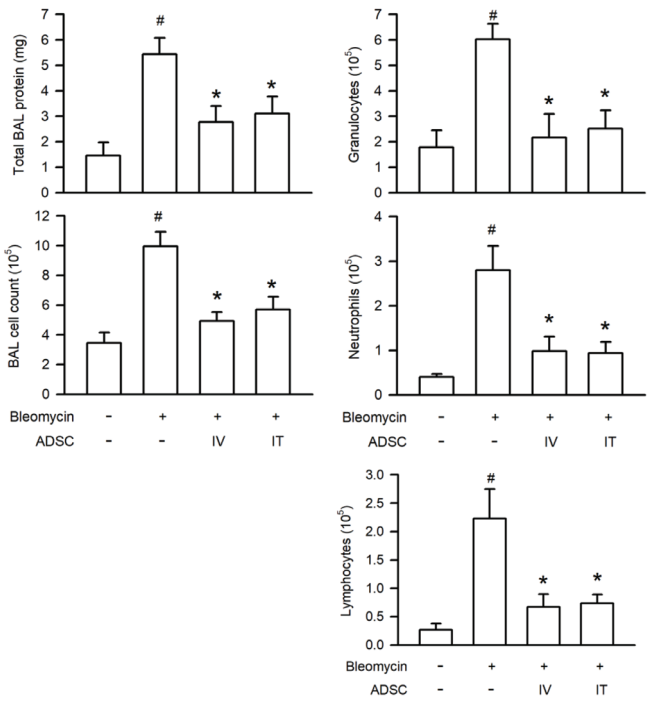


Fig.6: Effects of ADSC on the alveolar barrier dysfunction and leukocytic infiltration in bleomycin-induced pulmonary fibrosis. The parameters illustrated were leakage of protein and infiltration of leukocytes, including neutrophils and lymphocytes. Data are presented as mean ± SD (n=6 per group). Statistical significance was assessed using one-way ANOVA followed by Fisher's LSD test. The symbol # denoted a significant difference between the indicated group and the control group, while * indicated a significant difference between the indicated group and the bleomycin group, with P≤0.001. ADSC; Adipose-derived stem cells, IV; Intravenous, IT; Intratracheal, and BAL; Bronchoalveolar lavage.

Discussion

The majority of the studies that have investigated temporal trends in the incidence of IPF have identified an increasing trend for IPF incidence over time. Investigations conducted in the 1980s recorded somewhat low incidence rates, whereas subsequent studies using analogous datasets have identified significantly higher incidence rates for IPF. Such increases in incidence rates for IPF have been identified in the United Kingdom, South America, Asia, and Europe (2, 23).

Epidemiological studies in North America and Europe have reported that the annual incidence of IPF varies between 2.8 and 19 cases per 100,000 individuals. A retrospective analysis of at-risk adults in northern California from 2000 to 2014 utilised a common case-finding algorithm to estimate the incidence rate of IPF; the results revealed that the incidence rate was 6.8 per 100,000 person-years. However, when a modified algorithm with enhanced predictive value was employed, the incidence rate decreased to 5.6 per 100,000 individuals. In Europe, the United Kingdom has the highest IPF incidence rates, with the annual incidence ranging between 4.6 and 8.65 cases per 100,000 individuals and approximately 6000 new diagnoses made each year. By contrast, lower incidence rates, that is, rates of 1.3 to 4.3 and 4 to 6 per 100,000 person-years, have respectively been reported in Scandinavia and Russia. Globally, the lowest incidence rates of IPF are those in Asian countries; for example, South Korea, Taiwan, and Japan have annual incidence rates ranging from 1.2 to 4.16 cases per 100,000 individuals (2, 23, 24). Although 2 recently introduced antifibrotic drugs, namely, pirfenidone and nintedanib, have significantly mitigated the lung function decline associated with IPF, no cure has been developed for the disease. Thus, novel therapeutic approaches to IPF treatment should be developed. ADSCs are an essential component of stem cell-based therapy and have been one of the most widely used types of stem cells for >5 years in clinical settings. These cells have many advantages. For example, the number of ADSCs per volume of tissue and their proliferation rate are high. Moreover, they have been demonstrated to have antifibrotic, antiapoptotic, anti-inflammatory, and immunomodulatory properties and paracrine mechanisms in several preclinical studies (25).

A study reported that male Swiss albino mice that received IV-administered human ADSCs on days 3, 6, and 9 post-BLM administration exhibited significant improvement in survival rates by day 24 relative to that in mice that received human ADSCs with BLM administration (26). Another study reported that the administration of BLM on day 1 followed by IV administration of mouse ADSC did not significantly influence the body weights of C57BL/6 mice (27). By contrast, IV administration of ADSCs on day 10 post-BLM administration significantly reversed the reduction of body weight resulting from the administration of BLM in the rats on days 14 and 21 (28). In the present study, we found that IV and IT administration of human ADSCs on day 14 post-BLM treatment significantly increased the survival rates of BALB/c mice by day 42. Furthermore, we discovered that IT administration of human ADSCs led to a greater improvement in the survival rate than IV administration did. The decrease in body weight mediated by BLM was reversed by IT and IV administration of human ADSCs. The superior survival observed with IT ADSC administration may reflect more effective local modulation of the pulmonary inflammatory microenvironment and alveolar-capillary barrier integrity, while minimizing systemic exposure or procedure-related stress associated with IV delivery, as both routes produced comparable antifibrotic and anti-inflammatory effects within lung tissue, consistent with the predominantly paracrine and context-dependent actions of ADSC (25). In addition, differences in systemic immunomodulatory effects between IV and IT delivery cannot be excluded and may contribute to route-dependent survival outcomes, although this was not directly assessed in the present study (25). Although IV delivery has been proposed to confer survival benefits through systemic immunoregulation or protection against extrapulmonary complications, such mechanisms were not directly supported by the survival patterns observed in the present study. These results indicate that ADSCs administered either intravenously or intratracheally can improve the survival rates and body weights of mice with IPF, and the effects were stable and

long-lasting. Within this context, the present findings indicate that the route of ADSC administration may differentially influence survival outcomes, while exerting comparable effects on fibrotic remodeling and inflammatory responses in established pulmonary fibrosis.

BLM-induced IPF manifests with several pathological features, including lung oedema, relative lung weight, collagen synthesis, and pulmonary fibrosis (29). The present study discovered that IV and IT administration of human ADSCs reversed lung oedema and relative lung weight by day 14 post-BLM administration; in addition, administration of human ADSCs significantly increased the survival rates of the BALB/c mice by day 42 (13). Moreover, IV administration of ADSCs improved BLM-induced histopathological changes. IV administration of ADSCs also improved BLM-induced pulmonary fibrosis and architecture loss by day 1 and day 10 post-BLM administration and significantly reversed the reduction in body weight resulting from BLM treatment by day 21 (27, 28). In addition, IV and IT administration of human ADSCs on day 14 post-BLM administration significantly reversed collagen accumulation, histopathological changes, pulmonary fibrosis, architecture loss, and survival rate in the BALB/c mice by day 42. These results indicate that ADSCs administered either intravenously or intratracheally effectively improve IPF by mitigating BLM-induced lung oedema and pathological features, including histopathological changes and fibrotic lesions.

In the pathogenesis of BLM-induced pulmonary fibrosis, TGF-β is released by damaged pulmonary epithelial cells and alveolar macrophages. TGF-β promotes the activation of fibroblasts, which then differentiate into myofibroblasts (30). α-SMA is a marker of myofibroblast differentiation and contractility (31). TGF-β also mediates the activation of myofibroblasts, with this resulting in excessive deposition of extracellular matrix, primarily collagen (30, 31). Hydroxyproline is a major amino acid in collagen, and hydroxyproline is a biochemical marker of the collagen content in pulmonary fibrosis (21). Increased levels of TGF-β, α-SMA, and hydroxyproline are correlated with histological fibrosis scores and the progression of lung tissue scarring (32, 33). In the current study, after IV injection of human ADSCs on the 3rd, 6th, and 9th days after BLM administration, the levels of hydroxyproline and TGF-β mRNA in the mice decreased by the 24th day (26). Another study reported that administering BLM on day 1 and subsequently intravenously administering mouse ADSCs resulted in a significant reduction in the levels of hydroxyproline and TGF-β and α-SMA mRNA in C57BL/6 mice (27). By contrast, IV administration of rat ADSCs on day 10 post-BLM administration significantly reduced the expression levels of TGF-β mRNA in rats on days 14 and 21 (28). In the current study, both IV and IT administration of human ADSCs on the 14th day after BLM administration significantly reduced the levels of hydroxyproline, TGF-β, and α-SMA in the lungs of the mice. This result suggests that ADSCs effectively alleviated BLM-induced IPF by decreasing the levels of hydroxyproline, TGF-β, and α-SMA.

Several cytokines and chemokines, particularly TNF-α, SDF-1, IL-6, and IL-1β, play crucial roles in the pathogenesis of BLM-induced IPF (34, 35). When BLM is administered to induce IPF, TNF-α and IL-1β levels increase in the early stage of the disease, thus promoting the recruitment of neutrophils, macrophages, and fibroblasts to the lung injury site (34, 36). In addition to increasing the levels of the fibrogenic mediator of TGF-β, these recruited cells release other proinflammatory cytokines, including TNF-α, SDF-1, IL-6, and IL-1β, causing inflammation (35). IL-6 is secreted shortly after, and it amplifies the inflammatory response while promoting fibroblast activation and differentiation into myofibroblasts (37). SDF-1, also named CXCL12, is a chemoattractant that recruits leukocytes and fibrocytes to the lung injury site. Thus, SDF-1 participates in aberrant lung tissue remodelling during fibrosis (34, 36). After IV administration of human ADSCs on Days 3, 6, and 9 after BLM treatment, the BLM-induced levels of TNF and IL-1β mRNA significantly decreased by day 24 (26). When BLM administration followed by IV administration of mouse ADSCs was performed on day 1, the TNF-α mRNA levels in C57BL/6 mice notably decreased (27). Notably, IV administration of ADSCs increased the levels of IL-1 and TNF-α induced by BLM (13). In the present study, administering human ADSCs intravenously and intratracheally on day 14 post-BLM treatment significantly decreased the levels of TNF-α, SDF-1, IL-6, and IL-1β in BALF. This finding indicates that ADSCs effectively reduced the levels of BLM-induced fibrotic markers, such as TGF-β and α-SMA, by reducing the levels of these cytokines.

The reduction in proinflammatory cytokines observed in this study is consistent with the predominantly paracrine mode of action attributed to ADSCs. Rather than requiring durable engraftment within injured tissue, ADSCs are known to secrete a broad spectrum of soluble mediators that modulate macrophage polarization, suppress excessive cytokine release, and stabilize endothelial and epithelial barrier function (25). Although transient homing of administered cells to injured lung tissue may occur, accumulating evidence indicates that therapeutic effects can be achieved with minimal long-term cell retention. Moreover, ADSC-derived extracellular vesicles, including exosomes, have been increasingly recognized as functional mediators capable of transferring regulatory microRNAs and proteins that influence inflammatory and fibrotic signaling, thereby offering a plausible mechanistic explanation for the cytokine modulation observed in the present model (25, 38).

Alveolar barrier dysfunction is the initiating factor in the development of IPF induced by BLM because it leads to damage to alveolar epithelial cells, particularly type I and type II pneumocytes (39). The greater permeability of the alveolar-capillary barrier cause by BLM treatment results in plasma protein leakage and peripheral leukocyte infiltration into the alveolar space, exacerbating lung injury and promoting fibrotic processes (40). In addition, the

recruitment and activation of lymphocytes and granulocytes, such as neutrophils and macrophages, play pivotal roles in the inflammatory response and subsequent fibrotic remodelling in BLM-treated lung tissue (40). In the present study, we demonstrated that BLM-induced leakage of proteins and infiltration of leukocytes, such as granulocytes, neutrophils, and lymphocytes, into the alveolar space were reduced when human ADSCs were intravenously or intratracheally administered on day 14 post-BLM treatment. Notably, the absence of increased leukocyte infiltration in the IV group compared with the IT group further argues against a xenogeneic immune response to human ADSCs trapped in pulmonary capillaries.

Several limitations of the present study should be acknowledged. First, this work was conducted using a bleomycin-induced pulmonary fibrosis mouse model, which, although widely accepted, does not fully recapitulate the complexity and chronic progression of human IPF. Second, while survival, fibrotic remodeling, and inflammatory parameters were comprehensively evaluated, the biodistribution, long-term engraftment, and fate of administered ADSCs were not directly assessed. Third, potential differences in systemic immunomodulatory effects between IV and IT administration were not directly measured and therefore cannot be definitively distinguished in this study. In addition, some downstream mechanistic pathways, including extracellular vesicle-mediated signaling, were inferred based on existing literature rather than experimentally interrogated. Finally, as a preclinical study, the translational relevance of these findings requires further validation in well-designed clinical investigations.

From a clinical translation perspective, it is important to note that the therapeutic effects observed in this study are not unique to ADSCs, as bone marrow- and umbilical cord-derived MSCs share core immunomodulatory and paracrine properties. The use of ADSCs in the present work is therefore based on considerations of accessibility, scalability, and translational feasibility, rather than an assumption of biological superiority over other MSC sources (25). From a translational perspective, IV administration remains the most commonly used and clinically established route for stem cell–based therapies, owing to its procedural simplicity, reproducibility, and existing safety monitoring frameworks, whereas IT delivery is less standardized and typically requires bronchoscopic guidance. Although IV delivery may be associated with potential risks related to pulmonary microvascular trapping or first-pass cell sequestration in the lung, IT administration allows more localized deposition within the respiratory tract but may introduce procedure-related challenges and variability in distribution. Therefore, the selection of delivery route for clinical translation should balance therapeutic efficacy with feasibility and safety considerations. These perspectives are consistent with current clinical and translational evidence indicating that the therapeutic effects of adipose-derived or mesenchymal stem cells are predominantly paracrine and context dependent, rather than reliant on durable engraftment (25).

Conclusion

Our study demonstrated that IV administration of human ADSCs significantly reduced mortality in mice with BLM-induced IPF, with IV administration outperforming IT administration. Nevertheless, administration of ADSCs through either route effectively mitigated BLM-induced weight loss, with the outcomes being comparable between the routes. Histological analyses revealed that both ADSC(IV) and ADSC(IT) treatment significantly attenuated collagen synthesis, collagen fibre proliferation, and collagen fibre accumulation. The levels of hydroxyproline and profibrotic markers, such as TGF-β and α-SMA, were significantly reduced in both treatment groups, with no significant differences between the 2 administration routes. Additionally, both treatments led to decreases in the levels of inflammation-associated cytokines and the infiltration of leukocytes, improving alveolar barrier function. These findings highlight the therapeutic potential of ADSCs for alleviating pulmonary fibrosis and inflammation, irrespective of the administration route.

Acknowledgements

The authors would like to thank the National Science and Technology Council, Taiwan, for financially supporting this research under Contract No. NSTC 113-2320-B-040-014-MY3. We also thank the Chung-Kang Branch of the Cheng Ching General Hospital Research Fund (CH11100269A).

Conflict of Interest

There is no conflict of interest in this study. Dr. Tai Ping Lee and Dr. Martin Sieber are employees of BIONET Therapeutics Corp., which partially supported this study, contributed to early-stage conceptualization and study design, and provided the M.Sc. products used. However, the overall experimental plan and scientific interpretation were independently developed and overseen by the corresponding authors, Dr. Yu-Hsiang Kuan and Dr. Thomas Chang-Yao Tsao. Drs. Lee and Sieber had no role in data acquisition, statistical analysis, or manuscript preparation.

Authors' Contributions

Y.-L.N., Y.-H.K.; Conceptualization, Investigation, Writing-Rreview, Editing, Supervision, Project administration, and Funding acquisition. H.-T.S., C.-Y.L.; Methodology and Validation. M.S.; Resources and Data curation. Y.-Y.N., C.-Y.C., C.-C.T., C.-Y.T.T.; Data curation, Formal analysis, and Writing-original draft. All authors read and approved the final manuscript.

References

1. Moss BJ, Ryter SW, Rosas IO. Pathogenic mechanisms underlying idiopathic pulmonary fibrosis. Annu Rev Pathol. 2022; 17: 515-546. doi: 10.1146/annurev-pathol-042320-030240
2. Hutchinson J, Fogarty A, Hubbard R, McKeever T. Global incidence and mortality of idiopathic pulmonary fibrosis: a systematic review. Eur Respir J. 2015; 46(3): 795-806. doi: 10.1183/09031936.00185114
3. Wuyts WA, Agostini C, Antoniou KM, Bouros D, Chambers RC, Cottin V, et al. The pathogenesis of pulmonary fibrosis:

a moving target. Eur Respir J. 2013; 41(5): 1207-1218. doi: 10.1183/09031936.0007301
4. Saito S, Alkhatib A, Kolls JK, Kondoh Y, Lasky JA. Pharmacotherapy and adjunctive treatment for idiopathic pulmonary fibrosis (IPF). J Thorac Dis. 2019; 11 Suppl 14: S1740-S1754. doi: 10.21037/jtd.2019.04.62
5. Miura Y, Lam M, Bourke JE, Kanazawa S. Bimodal fibrosis in a novel mouse model of bleomycin-induced usual interstitial pneumonia. Life Sci Alliance. 2021; 4(1): e202101059. doi: 10.26508/lsa.202101059
6. Liu P, Yang S, Wang Z, Dai H, Wang C. Feasibility and mechanism analysis of Shenfu injection in the treatment of idiopathic pulmonary fibrosis. Front Pharmacol. 2021; 12: 670146. doi: 10.3389/fphar.2021.670146
7. Fytianos K, Schliep R, Mykoniati S, Khan P, Hostettler KE, Tamm M, et al. Anti-fibrotic effect of SDF-1β overexpression in bleomycin-injured rat lung. Pharmaceutics. 2022; 14(9): 1803. doi: 10.3390/pharmaceutics14091803
8. Tan JL, Lau SN, Leaw B, Nguyen HPT, Salamonsen LA, Saad MI, et al. Amnion epithelial cell-derived exosomes restrict lung injury and enhance endogenous lung repair. Stem Cells Transl Med. 2018; 7(2): 180-196. doi: 10.1002/sctm.17-0185
9. Zhang X, Zhang W, Chen X, Cai Y. Prevention of bleomycin-induced pulmonary inflammation and fibrosis in mice by bilobalide. Evid Based Complement Alternat Med. 2023; 2023: 1973163. doi: 10.1155/2023/1973163
10. Cossu G, Birchall M, Brown T, De Coppi P, Culme-Seymour E, Gibbon S, et al. Lancet commission: stem cells and regenerative medicine. Lancet. 2018; 391(10123): 883-910. doi: 10.1016/S0140-6736(17)31366-1
11. Zhang FQ, Jiang JL, Zhang JT, Niu H, Fu XQ, Zeng LL. Current status and future prospects of stem cell therapy in Alzheimer's disease. Neural Regen Res. 2020; 15(2): 242-250. doi: 10.4103/1673-5374.265544
12. Llontop P, Lopez-Fernandez D, Clavo B, Afonso Martin JL, Fiuza-Perez MD, Garcia Arranz M, et al. Airway transplantation of adipose stem cells protects against bleomycin-induced pulmonary fibrosis. J Investig Med. 2018; 66(4): 739-746. doi: 10.1136/jim-2017-000494
13. Jiang H, Zhang J, Zhang Z, Ren S, Zhang C. Effect of transplanted adipose-derived stem cells in mice exhibiting idiopathic pulmonary fibrosis. Mol Med Rep. 2015; 12(4): 5933-5938. doi: 10.3892/mmr.2015.4178
14. Lin SC, Panthi S, Hsuuw YH, Chen SH, Huang MJ, Sieber M, et al. Regenerative effect of mesenchymal stem cell on cartilage damage in a porcine model. Biomedicines. 2023; 11(7): 1810. doi: 10.3390/biomedicines11071810
15. Xin X, Yao D, Zhang K, Han S, Liu D, Wang H, et al. Protective effects of rosavin on bleomycin-induced pulmonary fibrosis via suppressing fibrotic and inflammatory signaling pathways in mice. Biomed Pharmacother. 2019; 115: 108870. doi: 10.1016/j.biopha.2019.108870
16. Yang L, Chen PP, Luo M, Shi WL, Hou DS, Gao Y, et al. Inhibitory effects of total ginsenoside on bleomycin-induced pulmonary fibrosis in mice. Biomed Pharmacother. 2019; 114: 108851. doi: 10.1016/j.biopha.2019.108851
17. Ni YL, Shen HT, Ng YY, Chen SP, Lee SS, Tseng CC, et al. Hibifolin protected pro-inflammatory response and oxidative stress in LPS-induced acute lung injury through antioxidative enzymes and the AMPK2/Nrf-2 pathway. Environ Toxicol. 2024; 39(7): 3799-3807. doi: 10.1002/tox.24233
18. Lee CY, Chen SP, Huang-Liu R, Gau SY, Li YC, Chen CJ, et al. Fucoxanthin decreases lipopolysaccharide-induced acute lung injury through the inhibition of RhoA activation and the NF-κB pathway. Environ Toxicol. 2022; 37(9): 2214-2222. doi: 10.1002/tox.23587
19. Yeh KL, Wu SW, Chiang CY, Chen CJ, Chen WY, Tseng CC, et al. Enhancing ocular protection against UVB: the role of irigenin in modulating oxidative stress and apoptotic pathways in vivo. Biomed Pharmacother. 2024; 179: 117346. doi: 10.1016/j.biopha.2024.117346
20. Xu Q, Liu H, Shi D, Fan X, Lv W, Jiang Y, et al. PGC-1α regulates endoplasmic reticulum stress in IPF-derived fibroblasts. Int Immunopharmacol. 2024; 138: 112514. doi: 10.1016/j.intimp.2024.112514
21. Liu N, Song Y, Liu T, Wang H, Yu N, Ma H. Metformin enhanced the effect of pirfenidone on pulmonary fibrosis in mice. Clin Respir J. 2024; 18(1): e13731. doi: 10.1111/crj.13731
22. Blin T, Parent C, Pichon G, Guillon A, Jouan Y, Allouchi H, et al. The proteolytic airway environment associated with pneumonia acts as a barrier for treatment with anti-infective antibodies. Eur J Pharm Biopharm. 2024; 195: 114163. doi: 10.1016/j.ejpb.2023.12.003
23. Olson AL, Gifford AH, Inase N, Fernandez Perez ER, Suda T. The epidemiology of idiopathic pulmonary fibrosis and interstitial lung diseases at risk of a progressive-fibrosing phenotype. Eur Respir Rev. 2018; 27(150): 180077. doi: 10.1183/16000617.0077-2018
24. Richeldi L, Collard HR, Jones MG. Idiopathic pulmonary fibrosis. Lancet. 2017; 389(10082): 1941-1952. doi: 10.1016/S0140-6736(17)30866-8
25. Sheykhhasan M, Wong JKL, Seifalian AM. Human adipose-derived stem cells with great therapeutic potential. Curr Stem Cell Res Ther. 2019; 14(7): 532-548. doi: 10.2174/1574888X14666190411121528
26. Reddy M, Fonseca L, Gowda S, Chougule B, Hari A, Totey S. Human adipose-derived mesenchymal stem cells attenuate early stage of bleomycin-induced pulmonary fibrosis: comparison with pirfenidone. Int J Stem Cells. 2016; 9(2): 192-206. doi: 10.15283/ijsc16041
27. Tashiro J, Elliot SJ, Gerth DJ, Xia X, Pereira-Simon S, Choi R, et al. Therapeutic benefits of young, but not old, adipose-derived mesenchymal stem cells in a chronic mouse model of bleomycin-induced pulmonary fibrosis. Transl Res. 2015; 166(6): 554-567. doi: 10.1016/j.trsl.2015.09.004
28. Felix RG, Bovolato ALC, Cotrim OS, Leao PDS, Batah SS, Golim MA, et al. Adipose-derived stem cells and adipose-derived stem cell-conditioned medium modulate in situ imbalance between collagen I- and collagen V-mediated IL-17 immune response recovering bleomycin pulmonary fibrosis. Histol Histopathol. 2020; 35(3): 289-301. doi: 10.14670/HH-18-152
29. Muri J, Durcova B, Slivka R, Vrbenska A, Makovicka M, Makovicky P, et al. Idiopathic pulmonary fibrosis: review of current knowledge. Physiol Res. 2024; 73(4): 487-497. doi: 10.33549/physiolres.935322
30. Jung E, Kim TY, Han J, Lee KY, Shin SY. TLR2-EGR1 signaling axis modulates TGF-β1-induced differentiation of fibroblasts into myofibroblasts in pulmonary fibrosis. Biochem Biophys Res Commun. 2024; 736: 150836. doi: 10.1016/j.bbrc.2024.150836
31. Wu P, Zhang W, Guan H, Jin T, Jia J, Luo B, et al. Macrophage erythropoietin signaling promotes macrophage-myofibroblast transformation and fibroblast-myofibroblast differentiation. Biochem Biophys Res Commun. 2024; 734: 150783. doi: 10.1016/j.bbrc.2024.150783
32. Liu Y, Chen H, Wu Y, Ai F, Li W, Peng H, et al. Sinomenine attenuates bleomycin-induced pulmonary fibrosis, inflammation, and oxidative stress by inhibiting TLR4/NLRP3/TGF-β signaling. Inhal Toxicol. 2024; 36(4): 217-227. doi: 10.1080/08958378.2024.2335193
33. Hao W, Yu TT, Zuo DZ, Hu HZ, Zhou PP. Stevioside attenuates bleomycin-induced pulmonary fibrosis by activating the Nrf2 pathway and inhibiting the NF-κB and TGF-β1/Smad2/3 pathways. Exp Lung Res. 2023; 49(1): 205-219. doi: 10.1080/01902148.2023.2286465
34. Fu S, Song X, Hu Y, Zhu Q, Lv X, Tang X, et al. Neotuberostemonine and tuberostemonine ameliorate pulmonary fibrosis through suppressing TGF-β and SDF-1 secreted by macrophages and fibroblasts via the PI3K-dependent AKT and ERK pathways. Chin J Nat Med. 2023; 21(7): 527-539. doi: 10.1016/S1875-5364(23)60444-3
35. Sanders M, Beringer P. Immunomodulatory activity of omadacycline in vitro and in a murine model of acute lung injury. mSphere. 2024; 9(1): e00671-24. doi: 10.1128/msphere.00671-24
36. Ma Z, Qiu L, Sun J, Wu Z, Liang S, Zhao Y, et al. A novel pulmonary fibrosis NOD/SCID murine model with natural aging. BMC Pulm Med. 2024; 24(1): 457. doi: 10.1186/s12890-024-03268-3
37. Yu W, Ye H, Li Y, Bao X, Ni Y, Chen X, et al. Pneumocystis carinii infection drives upregulation of Fn1 expression that causes pulmonary fibrosis with an inflammatory response. Rev Iberoam Micol. 2024; 41(1): 17-26. doi: 10.1016/j.riam.2024.04.002
38. Phinney DG, Pittenger MF. Concise review: MSC-derived exosomes for cell-free therapy. Stem Cells. 2017; 35(4): 851-858. doi: 10.1002/stem.2575
39. Rodriguez L, Tomer Y, Carson P, Dimopoulos T, Zhao M, Chavez K, et al. Chronic expression of a clinical SFTPC mutation causes murine lung fibrosis with idiopathic pulmonary fibrosis features. Am J Respir Cell Mol Biol. 2023; 68(4): 358-365. doi: 10.1165/rcmb.2022-0203MA
40. Araldi GL, Hwang YW, Raghu G. Development and evaluation of ABI-171, a new fluoro-catechin derivative, for the treatment of idiopathic pulmonary fibrosis. Int J Mol Sci. 2024; 25(21): 11827. doi: 10.3390/ijms252111827